Robust Loop Shaping Force Feedback Controller For Effective Force Testing

N. Nakata & E. Krug
Johns Hopkins University, USA

SUMMARY:
Effective force testing (EFT) is one of the force-based experimental methods for performance evaluation of structures that incorporate dynamic force control using hydraulic actuators. While previous studies have shown successful implementations of force control, controllable frequency ranges are limited to low frequencies (10 Hz). This study presents the EFT method using a robust loop shaping force feedback controller that can extend the frequency range up to 25 Hz. This study investigates the dynamic properties of hydraulic actuators and the design of a loop shaping controller that compensates for control-structure interaction as well as suppresses the effect of oil-column resonance. The designed loop shaping controller was successfully implemented into an EFT setup at the Johns Hopkins University. An experimental investigation was performed with linear and nonlinear test structures. Results showed that the loop shaping controller provided excellent force tracking performance as well as robustness for dynamic force loadings.

Keywords: Effective force testing, force control, hydraulic actuators, robust control, experimental methods

1. INTRODUCTION

One of the force-based experimental methods that has advantages over shake table tests and hybrid simulation is effective force testing (EFT). Idea of the EFT method was first introduced by Thewalt and Mahin (1987), and it is as follows. Dynamic performance of a structure can be evaluated by directly imposing a controlled force that is equivalent to the impact of an earthquake loading. Unlike shake table tests, EFT does not require shaking of the whole test structure. Therefore, EFT can be performed with smaller actuators than those required for shake table tests. Unlike hybrid simulation, the EFT method does not need to solve equations of motion; which is preferred since solution algorithms introduce numerical errors in simulation. A more detailed description of the EFT method can be found in Dimig *et al.* (1999).

While the EFT method is conceptually straight-forward, implementation is challenging. Due to the influence of the actuator piston velocity on the flow of oil in actuator chambers (i.e., natural velocity feedback), actuators do not have abilities to apply force at the natural frequencies of the test structure (Dyke *et al.* 1995). This phenomenon is called control-structure interaction, and it largely limits capabilities of the EFT method without proper compensations. Furthermore, because force measurement generally has a high level of noise, stability and robustness also become critical in force feedback control.

Several researchers have investigated dynamic force control through studies of the EFT method and force tracking problems. Dimig *et al.* (1999) verified the effect of control-structure interaction using a linear-elastic single-degree-of-freedom system. To compensate the control-structure interaction, an additional velocity feedback was suggested. Subsequently, Zhao *et al.* (2005) investigated nonlinear velocity feedback compensation for the control-structure interaction using the same test setup as Dimig, and experimentally verified their effectiveness. While these studies showed successful implementations of force control along with velocity feedback compensation, the bandwidth of the controlled force was limited to 10 Hz.

This paper presents effective force testing using a robust loop shaping force feedback controller. Loop shaping is a frequency domain technique for feedback control systems that can provide high performance and robustness as well as large bandwidth. Firstly, a brief overview of the effective force test method is presented. Following, a description of the experimental set up for EFT at Johns Hopkins University, a controller design using a loop shaping is discussed. Experimental investigation of the loop shaping force feedback controller is performed with linear and nonlinear test structures. Experimental results and observations are also presented in this paper.

2. EFFECTIVE FORCE TESTING

The governing equation of a single-degree-of-freedom system that is subjected to ground motion is expressed as:

$$m\left(\ddot{x}+\ddot{x}_g\right)+R\left(x,\dot{x}\right)=0 \qquad (2.1)$$

where m is the mass of the system; x is the relative displacement; $\ddot{x}_g$ is the ground acceleration; and $R\left(x,\dot{x}\right)$ is the nonlinear restoring force including viscous and elastic contributions. In the shake table tests, the ground motion is directly imposed by shaking the entire structure (see Figure 1). While the shake table tests are ideal for the evaluation of dynamic performance of structures, scale of the test structures are limited by capacities of the experimental facility.

The EFT method applies a dynamic force that is equivalent to the impact of the ground motion. The dynamic force is imposed on the structure at representative structural nodes. By reformulating the equation of motion in Eq (2.1), the governing equation in the EFT method can be written as:

$$m\ddot{x}+R\left(x,\dot{x}\right)=-m\ddot{x}_g=f_r \qquad (2.2)$$

where f_r is the reference force. It should be noted that although types of the input in the experiment are different, dynamics behind the shake table test and EFT methods are the same. Because the entire structure does not need to be shaken, the EFT method can be performed with smaller actuators than those required in shake table tests. Most importantly, nonlinear dynamic phenomenon including performance degradation and damage propagation, etc., can be evaluated at the true rate of the earthquake loading in the EFT method.

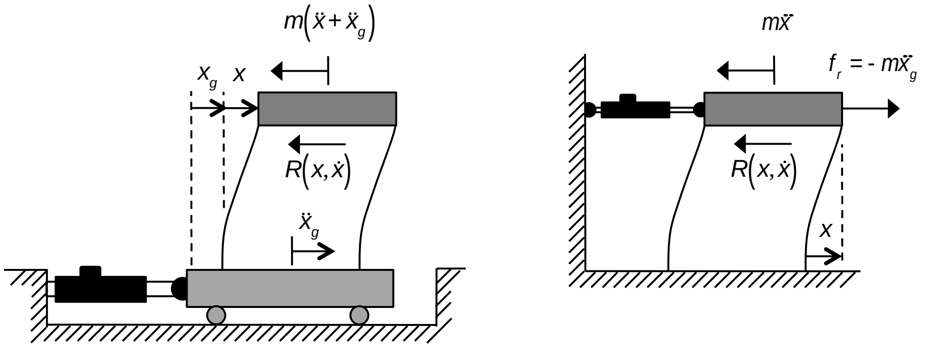

(a) Shake Table Test (b) Effective Force Test

Figure 1. Illustration of a shake table test and an effective force test of a SDOF system.

3. EXPERIMENTAL SETUP

This study employs an experimental setup in the Smart Structures and Hybrid Testing Laboratory at the Johns Hopkins University for the effective force tests with nonlinear test structures. Prior to the description of the force feedback controller in the next section, the experimental setup is presented. The experimental setup consists of a loading system, a control system and nonlinear test specimens.

3.1. Loading system

Figure 2 shows photos of the loading system for the effective force tests. A 1.2-meter W6 x 20 steel beam is used to represent a single-degree-of-freedom (SDOF) system. The beam has a pin joint at the base and is connected to a hydraulic actuator at the other end. The loading system is placed in a horizontal plane and the weight of the beam is supported by low friction wheels. With the maximum stroke of the actuator, 152mm, at the loading point, the loading system produces a rotation of 8.6 degree at the pin joint.

A restoring force of the SDOF system is developed by two steel rods that are bolted to plates at the pin connection; rotation of the pin joint results in tension and compression of the steel rods that generate a moment to resists the force by the actuator (see Figure 2). By imposing forces that exceed the capacity of the rods, nonlinear response of the SDOF system can be obtained. Because these rods are replaceable, this loading system allows for a great number of tests with structural nonlinearities including failure.

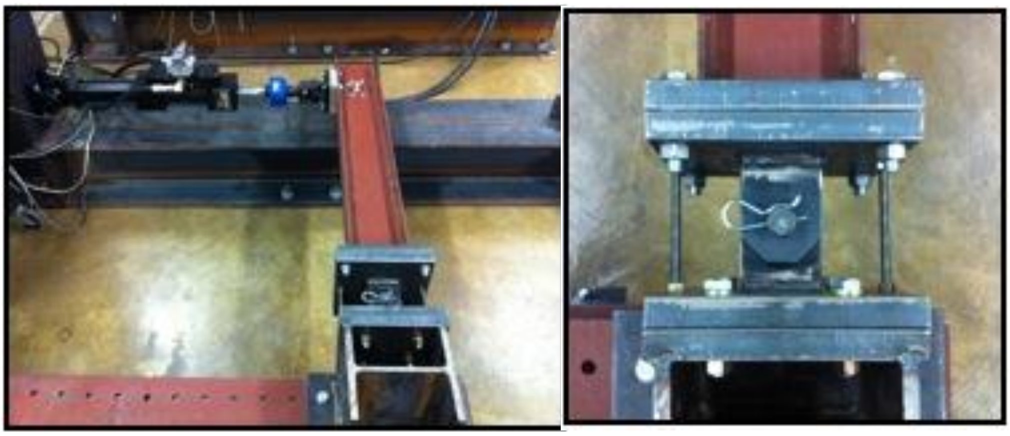

Figure 2. The nonlinear SDOF system that consists of a hydraulic actuator, a steel loading beam, a pin connection, two steel rods, and low-friction wheel.

3.2. Control system

The actuator utilized in the loading system is a 911D-series hydraulic actuator manufactured by Shore Western, Inc. It is equipped with a G761 series servo valve by Moog, Inc., a 22.2 kN load cell by Interface, Inc., and a 152mm DC operated linear variable differential transducer. Maximum stroke and dynamic force capacity of the actuator are 152 mm and 24.5 kN, respectively. The hydraulic power is supplied by a 114 litter-per-second Whisper Pak Model 160 from Shore Western, Inc. The hydraulic pressure is rated at 3000psi, and 3.8-litter accumulators are placed in both pressure and return lines to reduce the pressure drop.

A National Instruments PXI Express system is employed for integrated control and data acquisition processes. An embedded real-time controller, PXI-8031, allows analog-to-digital and digital-to-analog signal conversions at a sampling rate of 4 kHz. LabVIEW Real-Time is used as a software platform for the implementation of controller design in this study. For more details of hardware and software systems at the Smart Structures and Hybrid Testing Laboratory, refer to Nakata (2011).

4. FORCE FEEDBACK CONTROL WITH LOOP SHAPING

4.1. Force feedback control

Force feedback control compares the reference and measured forces and then generates the valve command based on the error between them. Figure 3 shows a block diagram of the closed-loop force feedback control including the input and measured noises. The dynamics of the closed-loop force feedback control system can be written in the Laplace domain as:

$$F_m = \frac{1}{1+C_f H_{fu}} \begin{bmatrix} C_f H_{fu} & H_{fu} & 1 \end{bmatrix} \begin{Bmatrix} F_r \\ W_u \\ W_f \end{Bmatrix} \tag{4.1}$$

where C_f is the force feedback controller; W_u is the Laplace transform of the input noise; W_f is the Laplace transform of the measurement noise; F_m is the Laplace transform of the measured force. The controller has to be designed such that it provides the desired performance in the complimentary sensitivity function $C_f H_{fu} / (1+C_f H_{fu})$ as well as robustness in the noise sensitivity function $C_f / (1+C_f H_{fu})$ and the sensitivity function $1/(1+C_f H_{fu})$.

Due to the control-structure interaction with hydraulic actuators, the transfer function from the voltage valve command, *u*, to the actuator force, *f*, has the denominator polynomials of the structural transfer function in the numerator as:

$$H_{fu} = \bar{H}_{fu} d_{xf} \tag{4.2}$$

where d_{xf} is the denominator polynomial of the transfer function of the structure. Because the roots of the denominator polynomials of the structural transfer function are the natural frequencies of the structure, this fact means that the valve command does not have the ability to control the actuator force at the natural frequencies of the structure unless d_{xf} are cancelled out in the force controller.

Substituting Eq (4.2) into the complementary sensitivity function, the transfer function from the reference force to the measured force can be expressed as:

$$H_f = \frac{F_m}{F_r} = \frac{C_f \bar{H}_{fu} d_{xf}}{1+C_f \bar{H}_{fu} d_{xf}} \tag{4.3}$$

It should be noted that the poles of the transfer function of the structure still appear as the zeros in the transfer function of the closed-loop force feedback control. This fact indicates that unless it is cancelled out by the force-feedback controller, the closed-loop does not have ability to generate force at the natural frequencies of the structure.

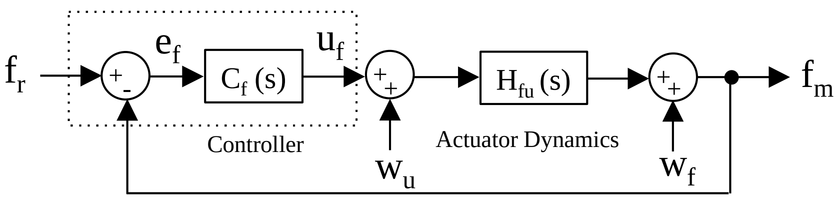

Figure 3. A block diagram of the closed-loop force feedback control system.

4.2. Loop shaping controller design

Loop shaping is a frequency domain technique for the design of feedback control systems. Based on the forms of a loop transfer function that is a product of the controller and the plant, the closed-loop feedback system can be designed to have desired performance and stability. In the case of force feedback control, the plant is the transfer function from the valve command voltage to the actuator force, H_{fu}, and thus, the loop transfer function is $C_f H_{fu}$. The key concept of the loop shaping is that the gain of the loop transfer function at low frequency must be large to have good tracking of the reference force while the gain at high frequency must be low to reject disturbances from the input and measurement noises.

In this study, in order to compensate for the control-structure interaction as well as to have a negative slope, the loop shaping force feedback controller is designed as:

$$C_f^{LS} = g / d_{xf} \tag{4.4}$$

where g is the gain for the loop shaping controller. The loop gain should be determined based on the crossover frequency.

4.3. Experimental transfer functions and loop shaping controller

Figure 4 shows the frequency response curve of the SDOF system and the frequency response curve of the open loop actuator dynamics from the voltage valve command to the actuator force. The frequency response of the structure shows a clear peak around 20Hz. This peak corresponds to the natural frequency of the SDOF system. The figure also shows an analytical SDOF model that fits the experimental data. The frequency response of the actuator shows a distinct drop around 20 Hz. This frequency coincides with the natural frequency of the structure, indicating the evidence of the control-structure interaction that is consistent with Eq 4.2.

Figure 5 shows the frequency domain characteristics of the loop-shaping controller designed for the SDOF system. The loop gain is selected as 25 so that the crossover frequency of the loop transfer function is around 10 Hz (see Figure 5 (b)). For the purposes of comparison, those of the conventional proportional controller where the gain is 0.0018 are also included in the plots. The transfer functions of the controllers show that the loop shaping controller has a peak at the natural frequency of the structure to compensate for the control-structure interaction. As the result of the pole-zero cancellation for the roots of the denominator polynomials of the structure transfer function in the loop shaping controller, the loop transfer function has a desirable form. On the other hand, the proportional controller has a distinct drop at the natural frequency of the structure and a relatively high gain at the high frequency range. It can be seen from the Nyquist plots in Figure 5 (c) that the loop shaping controller has larger gain margin than the proportional controller.

The overall transfer functions of the close-loop force feedback control are shown in Figure 5 (d). While the proportional controller is stable judging from the stability criterion, it cannot be practically employed because of its poor robustness that can cause vibration problems. On the other hand, the loop shaping controller provides excellent performance up to 15 Hz and rolls off beyond that range, indicating the robustness of the controller. Furthermore, unlike the proportional controller, the loop shaping controller compensates for the control-structure interaction at 20 Hz. It is clearly shown that the loop shaping controller designed based on Eq (4.4) meets requirements for the effective force test method. Therefore, the loop shaping force feedback controller designed here will be employed in a series of effective force tests with nonlinear test structures.

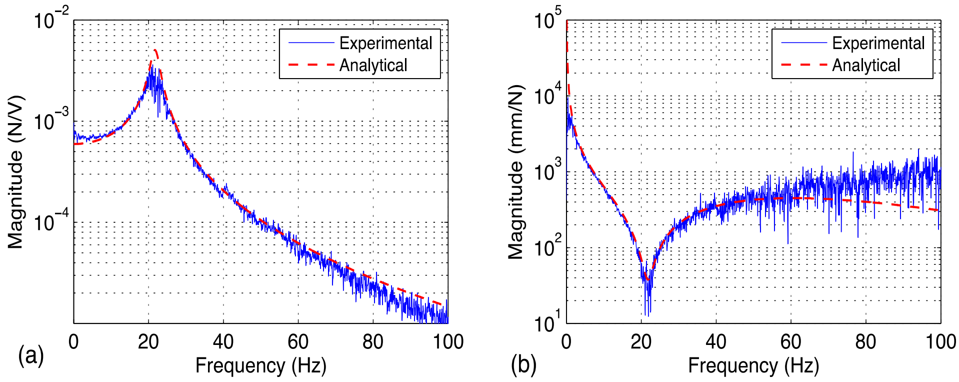

Figure 4. Frequency response curves: (a) structure; (b) actuator.

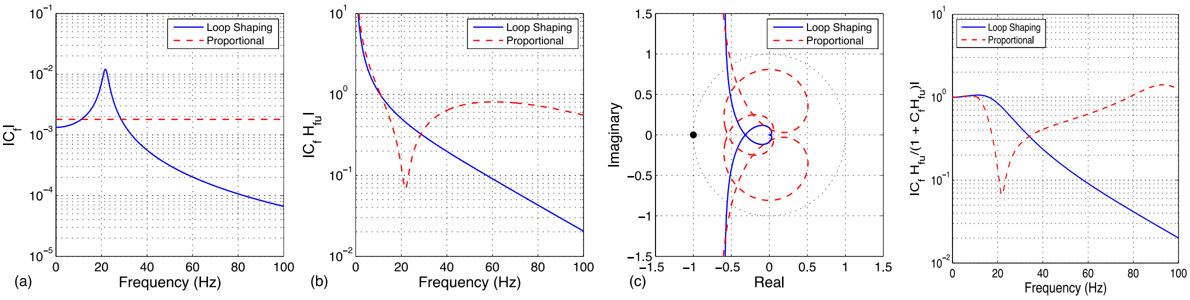

Figure 5. Frequency domain characteristics of the loop-shaping controller and the proportional controller: (a) controller transfer functions; (b) loop transfer functions; (c) Nyquist plots; (d) closed loop transfer functions.

5. EXPERIMENTAL VALIDATOIN OF DYNAMIC FORCE CONTROL

A series of effective force tests are conducted to investigate the capabilities of the loop shaping force-feedback controller with nonlinear test structures. Test results for the 1995 Kobe earthquake are presented in this paper. First, responses of the nonlinear SDOF system during the force controlled tests are discussed, and then, accuracy of dynamic force control is evaluated.

Figure 6 shows test results for three different force levels of the 1994 Northridge earthquake ground motion recorded at the Canoga station. In the force controlled test series, the dynamic force level is scaled up in sequence from a small level to a large one that is sufficient to cause failure of the test specimen. At the smallest force level of the three (the maximum reference force of 4448N), the measured force and the measured displacement are bounded within the linear ranges of 4500 N and 8 mm, respectively. As expected, the displacement-force relationship shows a typical linear elastic behavior. While the two rods at the base connection are bent during the test, they remained straight after the test and no observable damage was found.

At the reference force level of 6005N (b, e, and h), the measured force exceeds the linear range but reaches only 6000N, indicating that the target force level is greater than the capacity of the SDOF system. On the other hand, the measured displacement increases proportionally from the 4448N test and its maximum response reaches 10mm. It can be seen from the displacement-force relationship that while most of the loading cycles are still within the linear range at this level, a couple of cycles create hysteretic loops that result from the yielding of the SDOF system. Although significant residual displacement was not yet observed at this level, the two rods were bent during the test and they were not longer straight after the completion of the loading (see Figure 7 (a)).

At the reference force level of 7562 N (c, f, and i), the force peaks of each loading cycle become much higher than those in the previous two cases because of the amplification, but the measured force is still bounded within 6000 N. The measured displacement also exhibits a large response, reaching 40 mm. The SDOF system becomes highly nonlinear during the test and the center of vibration shifts from the zero position resulting in the residual displacement of 12mm. The displacement-force relationship in (i) shows that the level of force input is large enough to evaluate the nonlinear behavior of the SDOF system including the post peak response. Figure 7 (b) shows a photo of the two rods after the test of 8007 N. It can be seen that the two rods were completely buckled at the end of this test series.

Comparison of the forces and the force error ratio for the Kobe earthquake are shown in Figure 8. Excellent force tracking performance of the loop shaping controller can be seen for the reference force levels of 4448 N and 6005 N (a-d). For the reference force level of 7562 N, errors are more notable than the previous two levels due to the inability for the structure to generate the force beyond its capacity (e and f). Errors in the small force range in Figure 8 (f), especially after 8sec, are due to the yielding of the rods that are not captured in the design of the force feedback controller. While such inevitable errors exist, the test results demonstrate good performance and robustness of the loop shaping force feedback controller in the nonlinear effective force tests

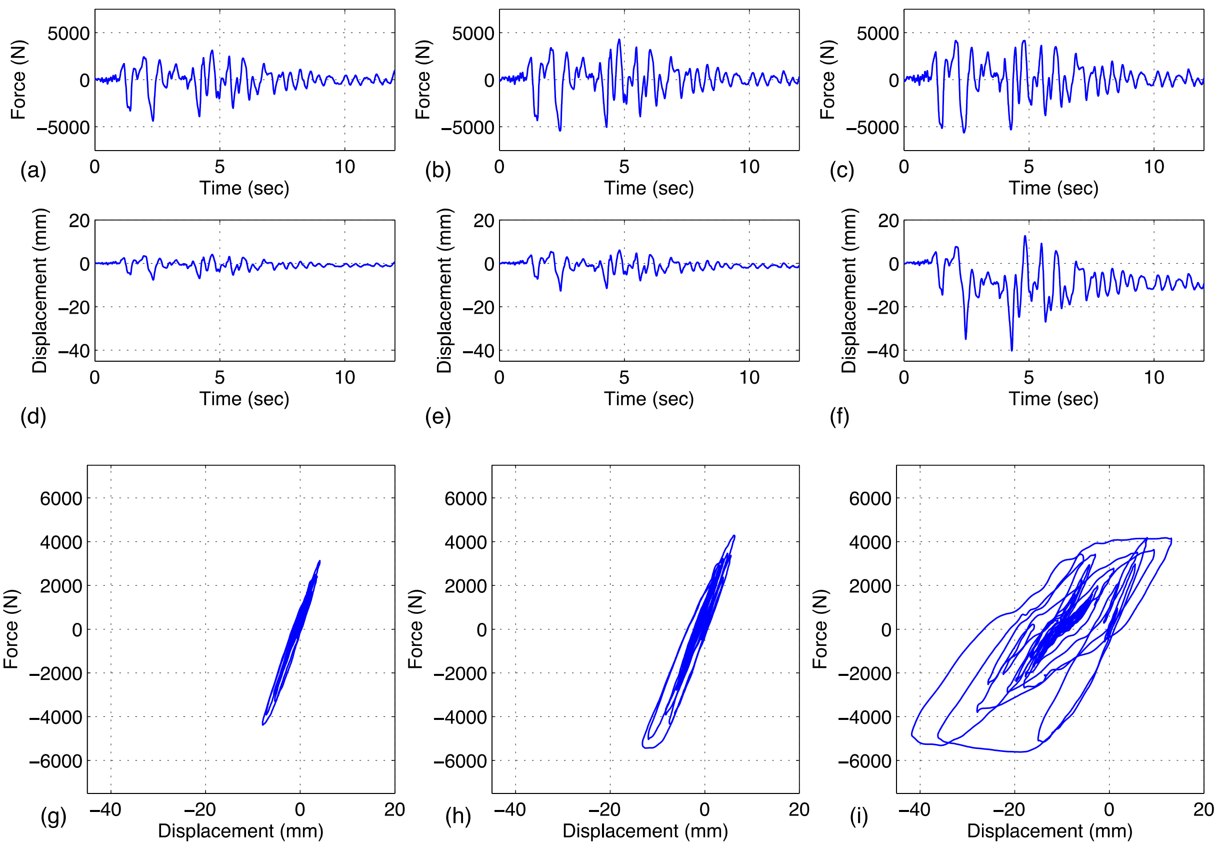

Figure 6. Effective force testing for the Kobe earthquake: (a) force for the peak excitation of 4448N; (b) force for the peak excitation of 6005N; (c) force for the peak excitation of 7562N; (d) displacement for the peak excitation of 4448N; (e) displacement for the peak excitation of 6005N; (f) displacement for the peak excitation of 7562N; (g) displacement-force relationship for the peak excitation of 4482N; (h) displacement-force relationship for the peak excitation of 6005N; and (i) displacement-force relationship for the peak excitation of 7562N.

Figure 7. Steel rods at different stages of the effective force test series; (a) after the test with the reference force level of 6005 N and (b) after the test with the reference force level of 7562 N.

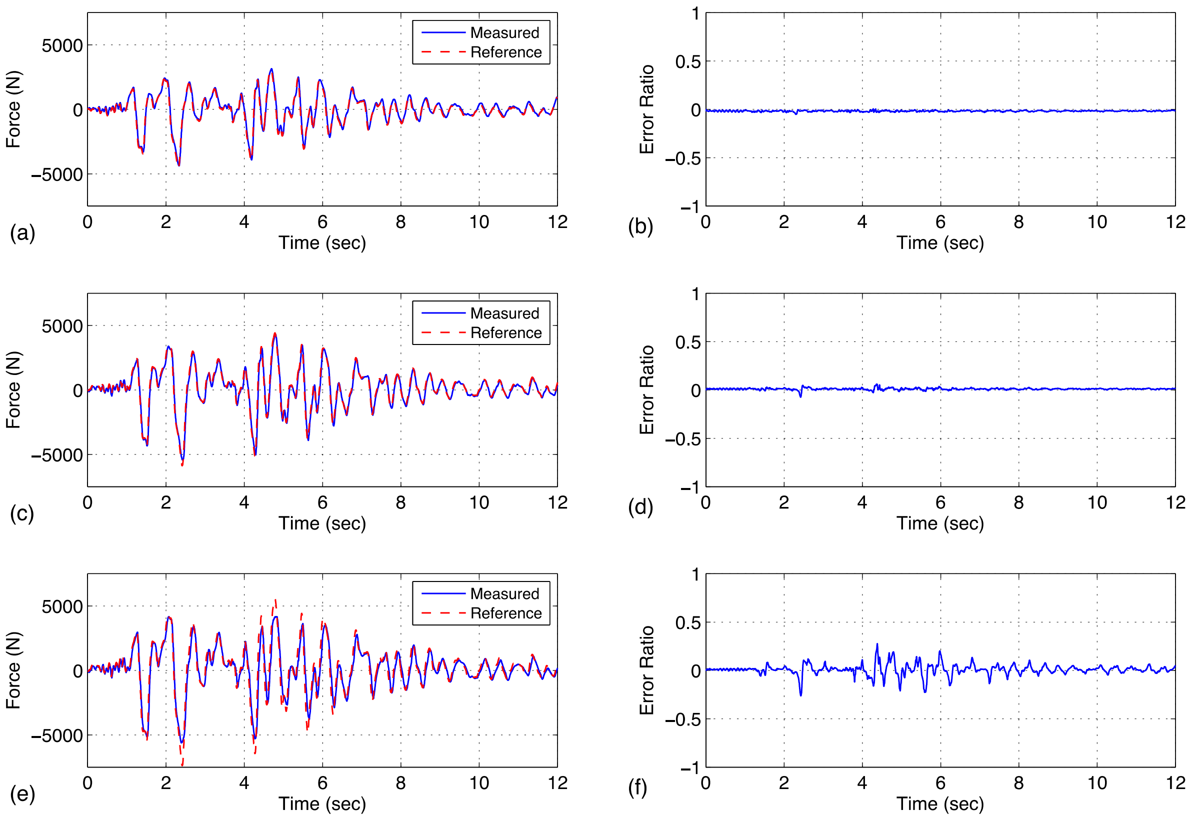

Figure 8. Comparison between the reference and measured forces, and force error ratio for the Kobe earthquake: (a) and (b) force and force error ratio for the peak excitation of 4448N, respectively; (c) and (d) force and force error ratio for the peak excitation of 6005N, respectively; (e) and (f) force and force error ratio for the peak excitation of 7562N, respectively.

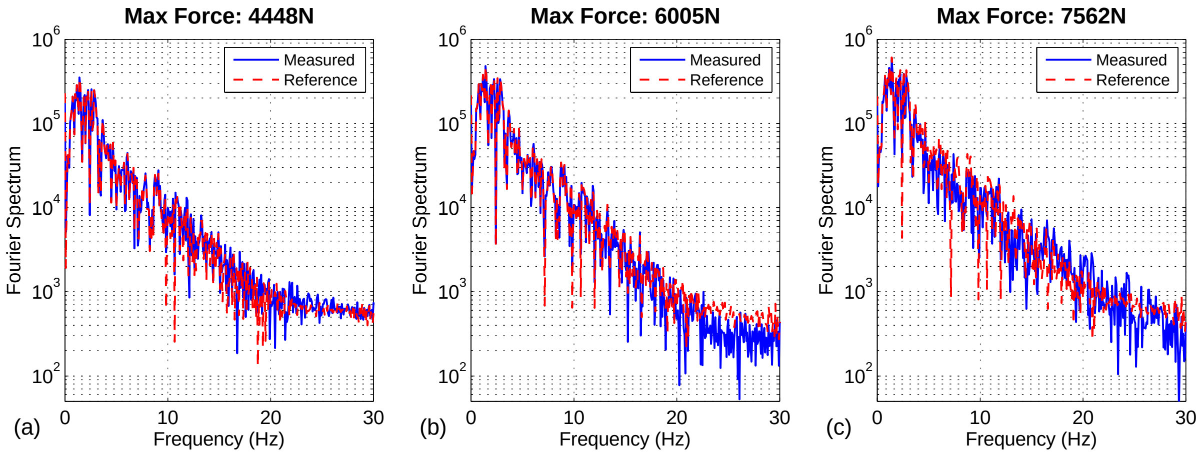

Figure 9. Fourier spectrum of the reference and measured forces for the Kobe earthquake: (a) reference force level of 4448 N; (b) reference force level of 6005 N; and (c) reference force level of 7562 N.

At last, control performance of the loop shaping controller is evaluated in the frequency domain. Figure 9 shows the Fourier spectrum of the reference and measured forces in the effective force test series for the Kobe earthquakes. For the reference force levels of 4448 N and 6005 N, the measured forces show a good agreement with the reference forces for almost all the frequency range. However, for the reference force level of 7562 N, a small discrepancy is spread over the entire frequency range. Overall, these Fourier spectra show good performance of the loop shaping controller in the frequency domain at all the levels

6. CONCLUSIONS

This paper presented an experimental verification of the effective force test method using a loop shaping force feedback controller with nonlinear test structures. A single-degree-of-freedom system with replaceable steel rods was employed as the nonlinear test specimen. A loop shaping controller was designed to compensate for the control-structure interaction and suppress the oil-column resonance of the actuator. Using the loop shaping force feedback controller, a series of effective force tests were conducted at the Johns Hopkins University.

Experimental results demonstrated that the effective force tests were successfully performed beyond the linear range of the SDOF system. It was shown that nonlinear hysteresis loops and residual displacements are developed in the force controlled tests. Judging through the time and frequency domain evaluations, the loop shaping controller was proven to provide high-performance force tracking capabilities as well as robustness despite the nonlinearities of the test structure. To the best of the author’s knowledge, the tests presented in this paper are the first effective force tests with structural nonlinearity beyond yielding and post-peak responses. With the loop shaping controller design, the effective force test method is now an accurate, stable and feasible force-based experimental method that can be applied to a various types of structures.

The authors are currently looking into the expansion of the effective force test method to multi-degrees-of-freedom systems. Such tasks require more research efforts including development of techniques to control dynamic forces of multiple actuators that are coupled through the test structures. The work presented in this paper lays the foundation for such challenging tasks. Any efforts, success and challenges in the force-based experimental methods by the authors will be shared with engineering community when they become available.

ACKNOWLEDGEMENT
This research is supported by the National Science Foundation under an award entitled "CAREER: Advanced Acceleration Control Methods and Substructure Techniques for Shaking Table Tests (grant number CMMI-0954958)".

REFERENCES

Astom, K.J. and Murray, R.M. (2006). "Feedback systems: an introduction for scientists and engineers", California Institute of Technology.

Dyke, S., Spencer, B., Quast, P., and Sain, M. (1995). "Role of control-structure interaction in protective system design", *Journal of Engineering Mechanics,* **121:2**, 322-338.

Dimig, J., Shield, C., French, C., Bailey, F., and Clark, A. (1999). "Effective force testing: a method of seismic simulation for structural testing", *Journal of Structural Engineering,* **125:9**,1028-1037.

Nakata, N. (2011). "A multi-purpose earthquake simulator and a flexible development platform for actuator controller design", *Journal of Vibration and Control,* available online.

Nakata, N. (2012). "Effective Force Testing Using A Robust Loop Shaping Controller", *Earthquake Engineering and Structural Dynamics* (Accepted).

Nakata, N. and Krug, E. (2012). "Validation of Effective Force Testing with Nonlinear Test Structures", ASCE *Journal of Engineering Mechanics,* submitted.

Thewalt, C.R. and Mahin, S.A. (1987). "Hybrid solution techniques for generalized pseudodynamic testing." *UCB/EERC-87/09,* University of California, Berkeley.

Zhao, J., French, C., Shield, C., and Posbergh, T. (2006). "Comparison of Tests of a Nonlinear Structure Using a Shake Table and the EFT Method", *Journal of Structural Engineering,* **132:9**, 1473-1481.